

RESEARCH REPORT

Rspo2 antagonizes FGF signaling during vertebrate mesoderm formation and patterning

Alice H. Reis and Sergei Y. Sokol*

ABSTRACT

R-spondins are a family of secreted proteins that play important roles in embryonic development and cancer. R-spondins have been shown to modulate the Wnt pathway; however, their involvement in other developmental signaling processes have remained largely unstudied. Here, we describe a novel function of Rspo2 in FGF pathway regulation *in vivo*. Overexpressed Rspo2 inhibited elongation of *Xenopus* ectoderm explants and Erk1 activation in response to FGF. By contrast, the constitutively active form of Mek1 stimulated Erk1 even in the presence of Rspo2, suggesting that Rspo2 functions upstream of Mek1. The observed inhibition of FGF signaling was accompanied by the downregulation of the FGF target genes *tbxt/brachyury* and *cdx4*, which mediate anterioposterior axis specification. Importantly, these target genes were upregulated in Rspo2-depleted explants. The FGF inhibitory activity was mapped to the thrombospondin type 1 region, contrasting the known function of the Furin-like domains in Wnt signaling. Further domain analysis revealed an unexpected intramolecular interaction that might control Rspo2 signaling output. We conclude that, in addition to its role in Wnt signaling, Rspo2 acts as an FGF antagonist during mesoderm formation and patterning.

KEY WORDS: Mesoderm, *Xenopus*, R-spondin, Erk1, Morphogenesis, *Cdx4*, *Brachyury*

INTRODUCTION

R-spondins are a family of four highly conserved secreted proteins (Rspo1-4) that play crucial roles during embryonic development and cancer (Aoki et al., 2007; de Lau et al., 2014; Kim et al., 2006; Raslan and Yoon, 2019). Mouse embryos lacking *rspo2*, encoding an R-spondin that is abundant in early embryogenesis, do not survive to term owing to lung, limb and craniofacial defects (Aoki et al., 2008; Bell et al., 2008; Nam et al., 2007; Yamada et al., 2009). Rspo2 has been also implicated in skeletogenesis (Tatsumi et al., 2014) and muscle development (Kazanskaya et al., 2004). Besides embryonic development, R-spondins are involved in stem cell survival (Kim et al., 2005; Sato et al., 2009) and multiple cancers. Approximately 10% of colorectal tumors were discovered to contain gene fusions involving *rspo2* and *rspo3*; these fusions were mutually exclusive with APC mutations (Seshagiri et al., 2012). Rspo2 has also been reported to modulate mammary tumorigenesis (Lowther et al., 2005; Theodorou et al., 2007). These observations

highlight the important functions of R-spondins, and specifically Rspo2, during early development and disease.

The functions of R-spondins have been mostly attributed to their ability to promote Wnt signaling (Bell et al., 2008; de Lau et al., 2014; Jin and Yoon, 2012; Kazanskaya et al., 2004). R-spondins upregulate Wnt signaling by preventing Frizzled receptor degradation when in complex with LGR4/5 and RNF43/ZNRF3 (Carmon et al., 2011; de Lau et al., 2011; Hao et al., 2012; Koo et al., 2012). R-spondins share a highly conserved structure comprising a signal peptide followed by two Furin-like domains (FU1 and FU2), a thrombospondin type 1 domain (TSP) and basic-rich (BR) amino acids in the C-terminal region (Jin and Yoon, 2012; Kim et al., 2006). The effect of R-spondins on the Wnt/ β -catenin pathway has been attributed to the Furin-like domains, whereas the TSP domain of Rspo3 has been shown to bind Syndecan4 and modulate non-canonical Wnt signaling (Ohkawara et al., 2011). The interaction of R-spondins with other signaling pathways remains poorly understood.

Several arguments suggest that the FGF pathway might be regulated by R-spondins. First, Rspo3 overexpression in *Xenopus* embryos produces blastopore closure defects (Ohkawara et al., 2011), mimicking the effect of a dominant-interfering FGF receptor (Amaya et al., 1991). Second, the TSP domain of Rspo3 interacts with syndecans and glypicans (Ohkawara et al., 2011), which are heparan sulfate proteoglycans (HSPGs) that function as co-receptors for FGF (García-García and Anderson, 2003; Rapraeger et al., 1991; Yayon et al., 1991). Third, the mouse embryos lacking the functions of FGF antagonists Spry2 and Spry4 (Taniguchi et al., 2007) exhibit similar defects to Rspo2-deficient embryos (Aoki et al., 2008; Bell et al., 2008; Nam et al., 2007; Yamada et al., 2009). Finally, Rspo3 knockdown upregulated Erk1 phosphorylation after osteogenic differentiation of human adipose-derived stem cells (Zhang et al., 2017). Together, these observations indicate that R-spondins might play a role in FGF signaling, in addition to their known function as Wnt modulators.

FGF signaling is initiated with the binding of the ligand to the tyrosine kinase receptors FGFR1-FGFR4. Tyrosine kinase stimulation leads to an intracellular signal transduction cascade that includes the activation of Ras and a series of cytosolic kinases, including Raf, Mek and Erk, ultimately leading to target gene transcription (Ornitz and Itoh, 2015; Patel and Shvartsman, 2018). Different FGF ligands have been shown to function in early mesoderm induction, central nervous system posteriorization, limb, lung, and heart, among other tissues, in vertebrate embryos, and have been implicated in cancer (Belov and Mohammadi, 2013; Ornitz and Itoh, 2015; Turner and Grose, 2010). In early embryogenesis, the FGF pathway is known to function in gastrulation and anteroposterior axis specification (Dorey and Amaya, 2010).

Taken together, this evidence prompted us to investigate whether Rspo2 has a role in FGF signaling during vertebrate embryonic

Department of Cell, Developmental and Regenerative Biology, Icahn School of Medicine at Mount Sinai, New York, NY 10029, USA.

*Author for correspondence (sergei.sokol@mssm.edu)

DOI: S.Y.S., 0000-0002-3963-9202

Handling Editor: Liz Robertson

Received 11 February 2020; Accepted 15 April 2020

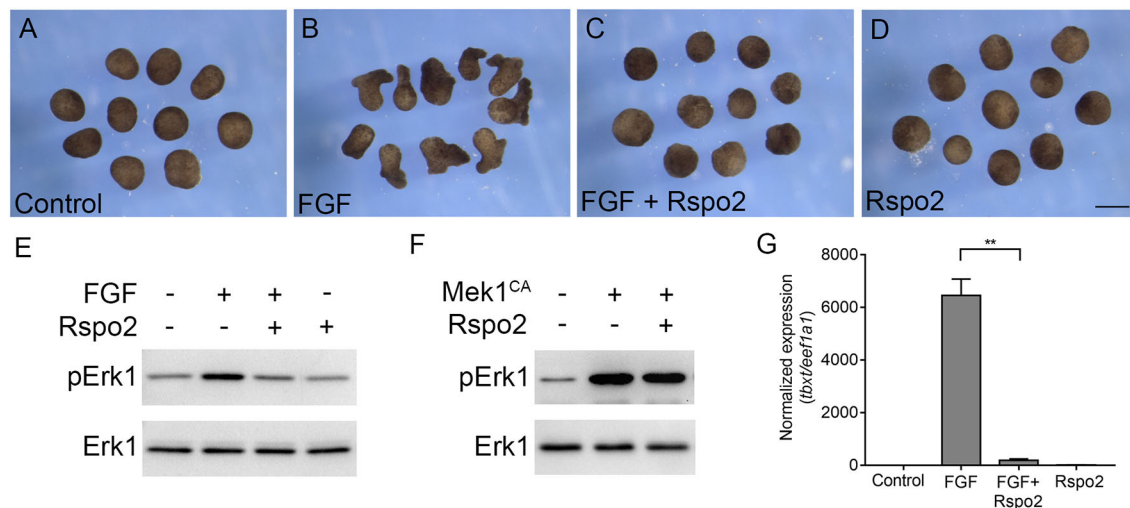


Fig. 1. Rspo2 inhibits ectoderm response to FGF but not MEK1. (A-G) Four-cell stage embryos were injected anally with Rspo2 RNA (0.5 ng) and Mek1^{CA} RNA (12 pg), as indicated. Ectoderm explants were dissected at stage 8 and treated with 100 ng/ml FGF2 protein. When control embryos reached stage 13, the explant morphology was imaged (A-D) or lysed for immunoblot or RT-qPCR analysis (E-G). (A) control uninjected ectoderm explants. (B) FGF-treated explants. (C) Rspo2-expressing explants stimulated with FGF. (D) Rspo2-expressing explants. Ten ectoderm explants were used per group in each experiment. The experiments were repeated five times. (E,F) Modulation of Erk1 activation by Rspo2. Immunoblotting was carried out with the antibodies against pErk1 and total Erk1. Data represent three to five independent experiments. (G) Rspo2 inhibits FGF-dependent induction of *tbxt*. RT-qPCR analysis was performed for *tbxt* and normalized by *eefta1*. The graph shows a representative experiment with triplicate samples from three independent experiments. Data are means \pm s.d. Statistical significance was assessed by Student's *t*-test. ***P* < 0.05. Scale bar: 300 μ m.

development. We used *Xenopus* early embryos, in which Rspo2 is abundantly expressed in the marginal zone during gastrulation and might therefore regulate FGF signaling during mesoderm formation (Kimelman and Kirschner, 1987; Slack et al., 1987). We show that Rspo2 inhibits FGF-mediated mesoderm specification and posterior patterning. These antagonistic effects of Rspo2 are mediated by the TSP domain upstream of the FGF receptors. Based on our analysis, we further propose that this inhibitory activity is modulated by an intramolecular interaction in Rspo2.

RESULTS AND DISCUSSION

Rspo2 blocks FGF signaling

Microinjection of Rspo2 RNA into two dorsal blastomeres of four-cell *Xenopus* embryos produced blastopore closure defects and subsequent tail truncations that were reminiscent of the phenotype obtained with a dominant interfering mutant of the FGF receptor 1 (Amaya et al., 1991) (Fig. S1), suggesting that Rspo2 may antagonize the FGF pathway. To investigate whether Rspo2 can modulate FGF signaling, we assessed mesoderm induction in ectoderm explants treated with FGF2 (Kimelman and Kirschner, 1987; Slack et al., 1987). Upon FGF2 stimulation, these explants acquire mesodermal cell fates and undergo extensive morphogenetic movements that are characteristic of the mesoderm during gastrulation. We observed that control explants developed as expected into atypical epidermis, whereas FGF2-treated explants had elongated by the time corresponding to the end of gastrulation (Fig. 1A,B). The injection of Rspo2 RNA prevented explant elongation (Fig. 1C). In the absence of FGF2, the morphology of the Rspo2-expressing explants was indistinguishable from untreated control explants (Fig. 1D). These observations indicate that Rspo2 prevented the elongation response of the cells to FGF2. Furthermore, Rspo2 inhibited FGF-dependent phosphorylation of Erk1, a downstream signaling target (LaBonne et al., 1995; Umbhauer et al., 1995) (Fig. 1E). These findings demonstrate that Rspo2 is a negative regulator of FGF2 signaling.

To determine which level of the FGF pathway is affected by Rspo2, we investigated whether Rspo2 inhibits the effect of the active form of Mek1 (Mek1^{CA}), an upstream activator of Erk1 (Cowley et al., 1994; Umbhauer et al., 1995). Mek1^{CA} upregulated Erk1 phosphorylation even in the presence of Rspo2, suggesting that Rspo2 functions upstream of Mek1 (Fig. 1F).

Finally, we evaluated the expression of *tbxt/brachyury*, a direct FGF target gene (Smith et al., 1991), in FGF2-stimulated ectoderm explants. RT-qPCR demonstrated that *tbxt* expression was strongly inhibited by Rspo2 by stage 13. (Fig. 1G). Taken together, these results show that Rspo2 is an efficient antagonist of FGF signaling.

Enhanced FGF signaling in embryos deficient in Rspo2 function

As overexpressed Rspo2 inhibited FGF signaling in our experiments, we predicted that, conversely, Rspo2 loss-of-function should stimulate the FGF pathway. To test this possibility, we designed and validated a specific morpholino (MO) oligonucleotide (RMO^{ATG}) (Heasman et al., 2000) (Fig. S2A). Rspo2 is known to be expressed in the marginal zone that produces FGF-dependent mesoderm, consistent with Rspo2 being induced by FGF (Kazanskaya et al., 2004). Ectoderm explants were dissected from stage 8 control embryos or embryos injected with 10 ng of RMO^{ATG}. After stimulation with FGF2, we observed that Rspo2-depleted explants elongated more efficiently than the control FGF2-treated explants (Fig. 2A,B). The morphology of the Rspo2-depleted explants did not change. This result implies that the response of Rspo2-depleted cells to FGF is enhanced. Further supporting this conclusion, RT-qPCR showed an increase in the expression of *tbxt* in FGF-treated explants compared with the controls (Fig. 2C).

We also assessed a role for Rspo2 in the regulation of two other FGF target genes, *cdx4* (*Xcad3*) (Northrop and Kimelman, 1994) and *mesogenin* (*msgn1*) (Wittler et al., 2007), in the context of endogenous FGF signaling. RT-qPCR was performed for uninjected control or Rspo2-depleted dorsal marginal zone explants, in the absence of

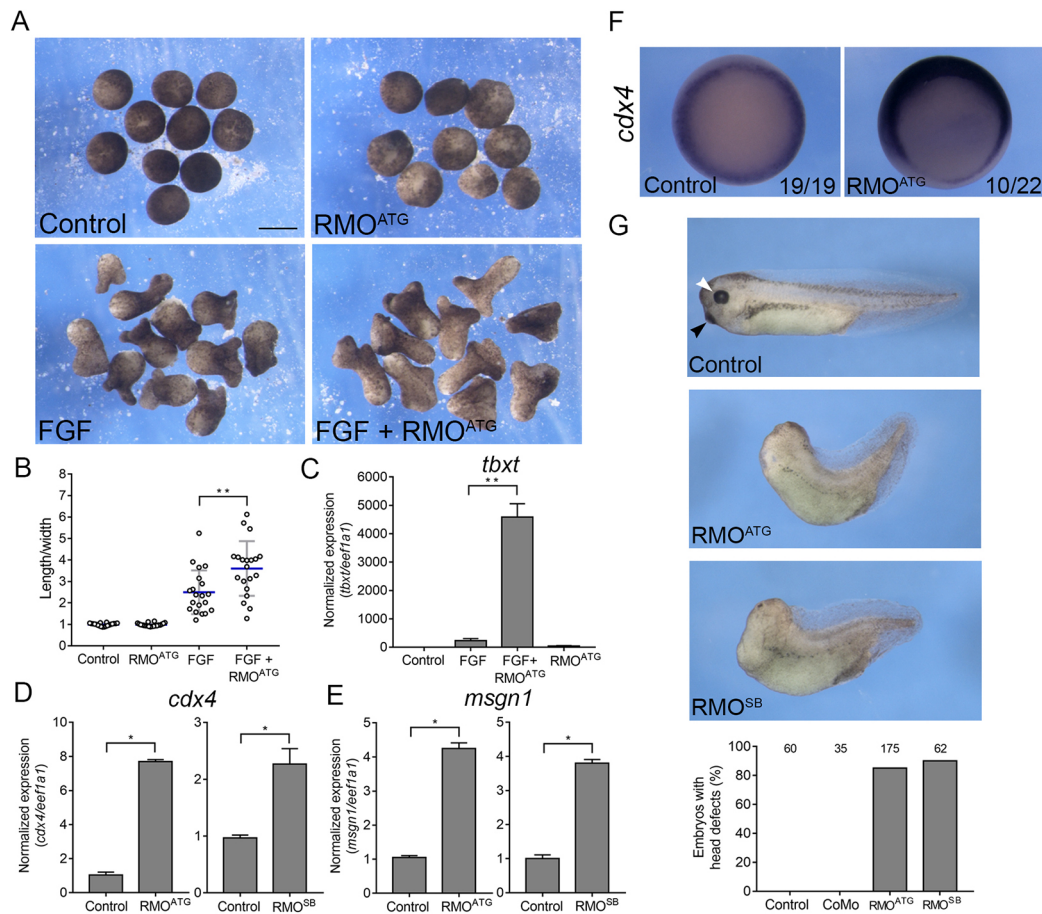


Fig. 2. Rspo2 depletion promotes FGF signaling. (A,B) Two-cell embryos were injected anally with RspoMO^{ATG} (10 ng) or RspoMO^{SB} (20 ng). Ectoderm explants were dissected at stage 8, treated with 25 ng/ml of FGF2 and cultured until stage 13. (A) Representative morphology of the embryos. (B) Quantification of the data in A, representative of two independent experiments. (C) RT-qPCR shows enhanced *tbxt* expression in FGF-stimulated ectodermal explants (stage 13) after Rspo2 depletion. (D,E) Enhanced *cdx4* and *msgr1* expression in the dorsal marginal zone (DMZ) explants depleted of Rspo2. RT-qPCR was carried out in stage 13 DMZ explants that were isolated at stage 10. Data are means±s.d. for triplicate samples. Graphs are representative of three independent experiments. (F) *In situ* hybridization with antisense *cdx4* probes was carried out with stage ≥10 control embryos and embryos injected marginally four times with 10 ng of RspoMO^{ATG}. The number of embryos with the displayed phenotype and the total number of injected embryos are shown. (G) Two dorsal animal blastomeres of four-cell embryos were injected with RMO^{ATG} or RMO^{SB} (10–20 ng each). Representative embryos are shown at stage 39. Arrowheads point to the eye (white) and the cement gland (black). The graph presents frequencies of embryos with head defects (missing eyes, cement gland and reduced facial structures). Numbers of embryos per group are shown at the top of each bar. Data are representative of three to four independent experiments. ***P*<0.01, **P*<0.05, Student's *t*-test. Scale bar: 300 μm.

exogenous FGF. RMO^{ATG} upregulated *cdx4* and *msgr1* transcript levels compared with controls (Fig. 2D,E). The same conclusion was reached with an independent splice-blocking morpholino (RMO^{SB}) (Fig. 2D,E; Fig. S2B). Whole-mount *in situ* hybridization also confirmed the upregulation of the *cdx4* expression domain in Rspo2 morphants (Fig. 2F). Embryos injected with either MO developed head truncations (Fig. 2G), consistent with FGF-mediated posteriorization. This phenotype is complementary to the posterior defects of embryos with overexpressed Rspo2. Together, these findings indicate that Rspo2 antagonizes FGF signaling during mesoderm patterning. Consistent with this conclusion, Rspo3 shRNA upregulated Erk1 phosphorylation after 14 days of osteogenic differentiation of human adipose-derived stem cells; however, the direct effect of Rspo3 on FGF signaling has not been evaluated (Zhang et al., 2017).

The TSP domain mediates the FGF inhibitory activity of Rspo2

We next sought to determine which Rspo2 domain mediates FGF inhibition. Several deletion constructs (Rspo2, RspoΔF and RspoΔT) that include different Rspo2 domains were made and

tested for the ability to interfere with FGF signaling in ectoderm explants (Fig. 3A). When introduced into early embryos, these constructs were all expressed at comparable levels (Fig. S3). Overexpression of Rspo2, RspoΔF or RspoΔT did not alter explant morphology on their own. However, upon FGF stimulation, Rspo2 and RspoΔF blocked explant elongation, indicating that the presence of the TSP domain correlates with the inhibitory activity (Fig. 3B–H). Unexpectedly, RspoΔT strongly enhanced elongation (Fig. 3I), suggesting that it might have a dominant interfering effect.

In agreement with the phenotypic analysis, Rspo2 and RspoΔF reduced Erk1 phosphorylation, whereas RspoΔT increased it (Fig. 3J). We next used SU5402, a specific inhibitor of FGF receptor activity (Fletcher and Harland, 2008; Mohammadi et al., 1997), to test whether the effects of RspoΔT on Erk1 require an FGF receptor. Indeed, SU5402 inhibited Erk1 phosphorylation caused by FGF2 in the presence of RspoΔT (Fig. 3K). This result is consistent with the effect of RspoΔT upstream of or parallel to the FGF receptor.

To ensure that Rspo2 is a specific antagonist of the FGF pathway, we tested whether it would interfere with Activin/Nodal/Smad2 pathway activation. Stimulation of ectoderm explants with Activin

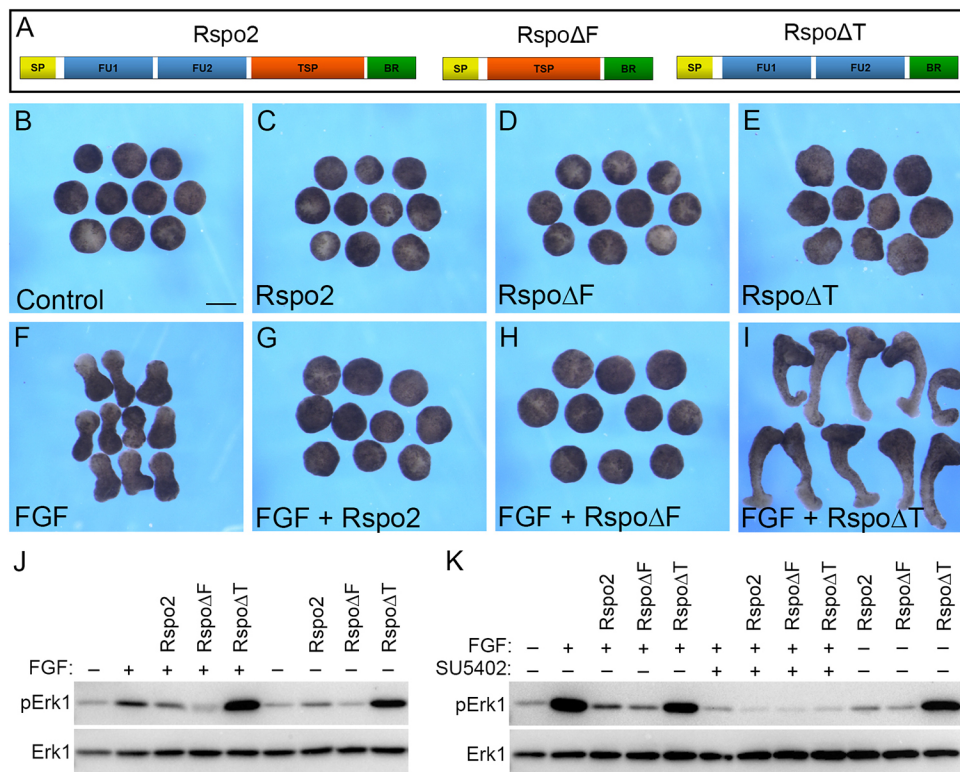


Fig. 3. Mapping FGF inhibitory activity to the TSP domain. (A) Schematic of Rspo2 constructs Rspo2, RspoΔF and RspoΔT. (B-E) Four-cell embryos were injected with 0.5 ng Rspo2, RspoΔF or RspoΔT RNA each, as indicated, and cultured until stage 8. Ectoderm explants were dissected, treated with 100 ng/ml of FGF2 with or without SU5402 (100 μM, final concentration), and cultured until stage 13. (B-I) Explant morphology is shown for unstimulated explants (B-E) and FGF2-stimulated explants (F-I). (J,K) Effects of Rspo2 constructs on FGF-dependent Erk1 activation. Immunoblot analysis was carried out with the antibodies against pErk1 and total Erk1. Scale bar: 300 μm.

A resulted in Smad2 phosphorylation, which was not altered by overexpressed Rspo2, RspoΔF or RspoΔT (Fig. S4).

Taken together, our experiments identify TSP as the domain responsible for the inhibitory effect of Rspo2 on FGF signaling.

Rspo domain interactions

In order to understand how the TSP domain blocks FGF signaling, we first examined whether RspoΔF or Rspo2 would interact with FGFR1. Our immunoprecipitation experiments did not show an interaction between these molecules (Fig. S5). As RspoΔT upregulated animal cap elongation and Erk1 activation in response to FGF, i.e. exhibited an effect opposite to the one in TSP, we next hypothesized that TSP activity is masked in Rspo2 by another protein domain. To test this possibility, two-cell embryos were co-injected with RspoΔF-GFP and RspoΔT-Flag RNAs. Co-immunoprecipitation analysis revealed the binding of RspoΔF-GFP to RspoΔT-Flag (Fig. 4A). Moreover,

full-length Rspo-GFP also associated with RspoΔT-Flag (Fig. 4B), indicating that both intramolecular and intermolecular interactions might contribute to Rspo2 signaling. Currently, we cannot exclude the potential contribution of the C-terminus retained in our constructs to the observed interaction.

These experiments reveal a novel domain interaction in Rspo2 that might modulate its biological activity through an additional layer of regulation. This interaction allows us to propose that RspoΔT has a dominant interfering effect by binding to endogenous inhibitory TSP domains. Alternatively, the synergy of RspoΔT with FGF might be due to the interaction of RspoΔT with other signaling pathways, e.g. Activin/Nodal or Wnt signaling. So far, we have found no evidence for RspoΔT influencing Smad2 phosphorylation in response to Activin (Fig. S4). However, RspoΔT might cooperate with FGF by promoting Wnt signaling, consistent with the reported synergy of FGF and Wnt proteins (Christian et al., 1992). In support of this hypothesis, Rspo2

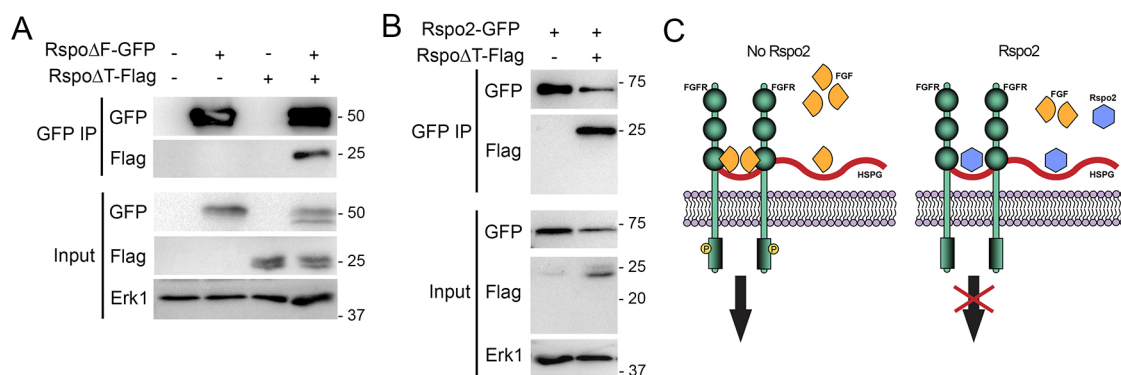


Fig. 4. The intramolecular interaction of protein domains in Rspo2. Four-cell stage embryos were injected with RNAs encoding RspoΔF-GFP, RspoΔT-Flag alone or co-injected. The embryos were cultured until stage 12 and lysed for GFP pulldown. (A) RspoΔT-Flag is co-immunoprecipitated (IP) by RspoΔF-GFP. (B) RspoΔT-Flag is co-immunoprecipitated by Rspo2-GFP. (C) Putative mechanistic model of FGF pathway inhibition by Rspo2. The association of Rspo2 with HSPGs prevents FGF ligand binding and signaling.

has been demonstrated to stimulate Wnt signaling via its FU-like domains (preserved in RspoΔT) by interfering with ZNRF3/RNF43, an inhibitor of Wnt signaling (Hao et al., 2012; Koo et al., 2012).

In addition to the previously studied role of R-spondins in Wnt signaling (Bell et al., 2008; de Lau et al., 2014; Jin and Yoon, 2012; Kazanskaya et al., 2004), this work demonstrates that Rspo2 acts as an antagonist of the FGF pathway during early embryonic development. At present, the mechanism underlying this function of Rspo2 remains unclear. Whereas the modulation of Wnt signaling by R-spondins involves the FU domains (Carmon et al., 2011; de Lau et al., 2011; Hao et al., 2012; Koo et al., 2012), the inhibitory activity of Rspo2 in FGF signaling is mediated by the TSP domain. So far, we could not detect any physical association of TSP with FGF ligands and receptors (Fig. S5). We propose that TSP inhibits FGF by sequestering HSPGs, which are essential FGF co-receptors (Rapraeger et al., 1991; Yayon et al., 1991) (Fig. 4C). In support of this possibility, both Rspo2 and Rspo3 have been reported to bind Syndecan4 and Glypican3 (Ohkawara et al., 2011). Further studies are needed to clarify the role of Rspo2 in the FGF pathway.

MATERIALS AND METHODS

Plasmids, *in vitro* RNA synthesis and morpholino oligonucleotides

The DNA clone 6988843 encoding *Xenopus tropicalis* Rspo2 was obtained from Dharmacon. The plasmids for expression of Rspo2 (pCS2-Rspo2-Flag or pCS2-Rspo2-Flag-GFP) was generated by inserting the coding region of Rspo2 sequence, amplified by PCR (Table S1), into the EcoRI and BamHI sites of pCS2-Flag or pCS2-Flag-GFP. Deletion mutants of Rspo2 (Table S1) constructs were generated using single primer-based site-directed mutagenesis as described previously (Itoh et al., 2005). pCS2-RspoΔF-Flag and pCS2-RspoΔF-GFP lack amino acids 37–134. pCS2-RspoΔT-Flag and pCS2-RspoΔT-GFP lack amino acids 147–204. All constructs were verified by Sanger sequencing. pCS2-Mek^{CA} was a gift from Stanislav Shvartsman (Princeton University, Princeton, NJ, USA). FGFR1-Flag plasmid was subcloned into pCS2 from a plasmid provided by P. Soriano (Icahn School of Medicine at Mount Sinai, New York, NY, USA).

Capped mRNAs were synthesized using an mMessage mMachine kit (Ambion). The following linearized plasmids were used as templates: pCS2-Rspo-Flag, pCS2-Rspo-Flag-GFP, pCS2-RspoΔF-Flag, pCS2-RspoΔF-GFP, pCS2-RspoΔT-Flag, pCS2-mFGFR1-Flag and pCS2-Mek^{CA}.

The following MOs were purchased from Gene Tools: RspoMO^{ATG}, 5'-AAAGAGTTGAACTGCATTTGG-3'; RspoMO^{SB}, 5'-GCAGCTG-GATACACAGAAACAAGA-3'; and control MO (CoMO), 5'-GCTTCA-GCTAGTGACACATGCAT-3'.

Xenopus embryo culture, microinjections, imaging and statistical analysis

In vitro fertilization and culture of *Xenopus laevis* embryos were carried out as described previously (Dollar et al., 2005). Frog handling was carried out according to the animal protocol approved by the Icahn School of Medicine at Mount Sinai Institutional Animal Care and Use Committee. Staging was determined according to Nieuwkoop and Faber (Nieuwkoop and Faber, 1967). For microinjections, four-cell embryos were transferred into 3% Ficoll in 0.5× Marc's Modified Ringer's buffer [50 mM NaCl, 1 mM KCl, 1 mM CaCl₂, 0.5 mM MgCl₂, 2.5 mM HEPES (pH 7.4)] (Peng, 1991) and 10 nl of mRNA or MO solution (10 ng of RspoMO^{ATG} and 20 ng of RspoMO^{SB}) was injected into one or more blastomeres. Control MO was injected at a dose that matched the highest dose of RspoMO used in the same experiment. Amounts of injected mRNA and MOs were optimized in preliminary dose-response experiments. Embryos were imaged at the indicated stages using a Leica Wild M10 stereomicroscope and the OpenLab software. Unless otherwise specified, all experiments were carried out at least three times. Statistical analyses were performed using GraphPad Prism 6 software. Data are mean±s.d. and an unpaired two-tailed Student's *t*-test was used to determine statistical significance (**P*<0.05; ***P*<0.01).

Ectoderm and marginal zone explants, and RT-qPCR

Two-to-four cell embryos were injected anally with Rspo2 RNA (0.5 ng). At stage 8, the ectodermal explants were dissected and treated with recombinant FGF2 at 25–100 ng/ml as described previously (Itoh and Sokol, 1994). SU5402 was added to the medium at 100 μM concentration, according to Fletcher and Harland (2008). The explants were cultured until the early neurula stage, at which point they were analyzed for morphology or harvested for western blot or RT-qPCR. Marginal zone explants were dissected at the early gastrula stage and cultured until stage 12.5, at which point they were lysed for RT-qPCR analysis.

For quantitative PCR (RT-qPCR), RNA was extracted from a group of ten animal caps or seven marginal zone explants at stage 12.5, using an RNeasy kit (Qiagen). cDNA was made from 1 μg of total RNA using iScript (Bio-Rad). qPCR reactions were amplified using a CFX96 light cycler (Bio-Rad) with Universal SYBR Green Supermix (Bio-Rad). Data represent at least three independent experiments performed in triplicate. Data are means±s.d. All samples were normalized to *efl1a1* expression and marker expression in control embryos. The primer sequences used for RT-qPCR are listed in Table S1.

For Activin A treatment, ectodermal explants were dissected at stage 8 and stimulated with 0.5 ng/ml of recombinant Activin A (Itoh and Sokol, 1994) for 30 min. Cell lysates were separated by PAGE and immunoblotted with anti-phospho-Smad2 (1:1000, Cell Signaling Technology, 3108) and mouse anti-FLAG M2 antibody (1:2000, Sigma-Aldrich, F3165).

Immunoprecipitation and immunoblot analysis, and whole-mount *in situ* hybridization

Immunoprecipitation was performed by using 30 embryos per condition. Embryos were injected at the four-cell stage with Rspo-ΔF-GFP, Rspo-ΔT-Flag or Rspo-Flag-GFP RNA. Embryos were lysed at stage 11 and GFP pulldown was carried out by incubating the lysates with GFP-Trap (Chromotek) according to the manufacturer's instructions. Immunoblot analysis was carried out as described previously (Itoh et al., 2005). Briefly, ten animal caps, cultured until the equivalent of stage 13, were homogenized in 50 μl of the lysis buffer [50 mM Tris-HCl (pH 7.6), 50 mM NaCl, 1 mM EDTA, 1% Triton X-100, 10 mM NaF, 1 mM Na₃VO₄, 25 mM β-glycerol phosphate, 1 mM phenylmethylsulfonyl fluoride]. After centrifugation for 3 min at 16,000 *g*, the supernatant was subjected to SDS-PAGE and immunoblotting. The following primary antibodies were used: mouse anti-FLAG M2 (1:2000, Sigma-Aldrich, F3165), mouse anti-GFP (1:1000, Santa Cruz Biotechnology, SC-9996) and rabbit anti-phospho-p44/42 MAPK (pErk1/2) (1:1000, Cell Signaling Technology, 4370S). Rabbit anti-Erk1 (1:1000, Santa Cruz Biotechnology, SC-94) staining was performed to provide a loading control. Chemiluminescence was captured by the ChemiDoc MP imager (BioRad).

Whole-mount *in situ* hybridization was carried out using standard techniques (Harland, 1991) with the digoxigenin-labeled antisense RNA probes for *cdx4* (Northrop and Kimelman, 1994).

Acknowledgements

We thank Phil Soriano and members of the Sokol laboratory for the critical reading of the manuscript.

Competing interests

The authors declare no competing or financial interests.

Author contributions

Conceptualization: A.H.R., S.Y.S.; Methodology: A.H.R., S.Y.S.; Validation: A.H.R.; Formal analysis: A.H.R.; Investigation: S.Y.S.; Resources: S.Y.S.; Writing - original draft: A.H.R., S.Y.S.; Writing - review & editing: A.H.R., S.Y.S.; Supervision: S.Y.S.; Funding acquisition: S.Y.S.

Funding

This study was supported by the Eunice Kennedy Shriver National Institute of Child Health and Human Development (HD092990 to S.Y.S.). Deposited in PMC for release after 12 months.

Supplementary information

Supplementary information available online at <http://dev.biologists.org/lookup/doi/10.1242/dev.189324.supplemental>

Peer review history

The peer review history is available online at <https://dev.biologists.org/lookup/doi/10.1242/dev.189324.reviewer-comments.pdf>

References

- Amaya, E., Musci, T. J. and Kirschner, M. W. (1991). Expression of a dominant negative mutant of the FGF receptor disrupts mesoderm formation in *Xenopus* embryos. *Cell* **66**, 257–270. doi:10.1016/0092-8674(91)90616-7
- Aoki, M., Mieda, M., Ikeda, T., Hamada, Y., Nakamura, H. and Okamoto, H. (2007). R-spondin3 is required for mouse placental development. *Dev. Biol.* **301**, 218–226. doi:10.1016/j.ydbio.2006.08.018
- Aoki, M., Kiyonari, H., Nakamura, H. and Okamoto, H. (2008). R-spondin2 expression in the apical ectodermal ridge is essential for outgrowth and patterning in mouse limb development. *Dev. Growth Differ.* **50**, 85–95. doi:10.1111/j.1440-169X.2007.00978.x
- Bell, S. M., Schreiner, C. M., Wert, S. E., Mucenski, M. L., Scott, W. J. and Whitsett, J. A. (2008). R-spondin 2 is required for normal laryngeal-tracheal, lung and limb morphogenesis. *Development* **135**, 1049–1058. doi:10.1242/dev.013359
- Belov, A. A. and Mohammadi, M. (2013). Molecular mechanisms of fibroblast growth factor signaling in physiology and pathology. *Cold Spring Harb. Perspect. Biol.* **5**. doi:10.1101/cshperspect.a015958
- Carmon, K. S., Gong, X., Lin, Q., Thomas, A. and Liu, Q. (2011). R-spondins function as ligands of the orphan receptors LGR4 and LGR5 to regulate Wnt/beta-catenin signaling. *Proc. Natl. Acad. Sci. USA* **108**, 11452–11457. doi:10.1073/pnas.1106083108
- Christian, J. L., Olson, D. J. and Moon, R. T. (1992). Xwnt-8 modifies the character of mesoderm induced by bFGF in isolated *Xenopus* ectoderm. *EMBO J.* **11**, 33–41. doi:10.1002/j.1460-2075.1992.tb05024.x
- Cowley, S., Paterson, H., Kemp, P. and Marshall, C. J. (1994). Activation of MAP kinase is necessary and sufficient for PC12 differentiation and for transformation of NIH 3T3 cells. *Cell* **77**, 841–852. doi:10.1016/0092-8674(94)90133-3
- de Lau, W., Barker, N., Low, T. Y., Koo, B.-K., Li, V. S., Teunissen, H., Kujala, P., Haegebarth, A., Peters, P. J., van de Wetering, M. et al. (2011). Lgr5 homologues associate with Wnt receptors and mediate R-spondin signalling. *Nature* **476**, 293–297. doi:10.1038/nature10337
- de Lau, W., Peng, W. C., Gros, P. and Clevers, H. (2014). The R-spondin/Lgr5/Rnf43 module: regulator of Wnt signal strength. *Genes Dev.* **28**, 305–316. doi:10.1101/gad.235473.113
- Dollar, G. L., Weber, U., Mlodzik, M. and Sokol, S. Y. (2005). Regulation of Lethal giant larvae by Dishevelled. *Nature* **437**, 1376–1380. doi:10.1038/nature04116
- Dorey, K. and Amaya, E. (2010). FGF signalling: diverse roles during early vertebrate embryogenesis. *Development* **137**, 3731–3742. doi:10.1242/dev.037689
- Fletcher, R. B. and Harland, R. M. (2008). The role of FGF signaling in the establishment and maintenance of mesodermal gene expression in *Xenopus*. *Dev. Dyn.* **237**, 1243–1254. doi:10.1002/dvdy.21517
- García-García, M. J. and Anderson, K. V. (2003). Essential role of glycosaminoglycans in Fgf signaling during mouse gastrulation. *Cell* **114**, 727–737. doi:10.1016/S0092-8674(03)00715-3
- Hao, H.-X., Xie, Y., Zhang, Y., Charlat, O., Oster, E., Avello, M., Lei, H., Mickanin, C., Liu, D., Ruffner, H. et al. (2012). ZNRF3 promotes Wnt receptor turnover in an R-spondin-sensitive manner. *Nature* **485**, 195–200. doi:10.1038/nature11019
- Harland, R. M. (1991). *In situ* hybridization: an improved whole-mount method for *Xenopus* embryos. In *Methods Cell Biol.* (ed. B. K. Kay and H. B. Peng), pp. 685–695. San Diego: Academic Press Inc.
- Heasman, J., Kofron, M. and Wylie, C. (2000). Beta-catenin signaling activity dissected in the early *Xenopus* embryo: a novel antisense approach. *Dev. Biol.* **222**, 124–134. doi:10.1006/dbio.2000.9720
- Itoh, K. and Sokol, S. Y. (1994). Heparan sulfate proteoglycans are required for mesoderm formation in *Xenopus* embryos. *Development* **120**, 2703–2711.
- Itoh, K., Brott, B. K., Bae, G.-U., Ratcliffe, M. J. and Sokol, S. Y. (2005). Nuclear localization is required for Dishevelled function in Wnt/beta-catenin signaling. *J. Biol.* **4**, 3. doi:10.1186/jbiol20
- Jin, Y.-R. and Yoon, J. K. (2012). The R-spondin family of proteins: emerging regulators of WNT signalling. *Int. J. Biochem. Cell Biol.* **44**, 2278–2287. doi:10.1016/j.biocel.2012.09.006
- Kazanskaya, O., Glinka, A., del Barco Barrantes, I., Stanek, P., Niehrs, C. and Wu, W. (2004). R-Spondin2 is a secreted activator of Wnt/ β -catenin signaling and is required for *Xenopus* myogenesis. *Dev. Cell* **7**, 525–534. doi:10.1016/j.devcel.2004.07.019
- Kim, K.-A., Kakitani, M., Zhao, J., Oshima, T., Tang, T., Binnerts, M., Liu, Y., Boyle, B., Park, E., Emtage, P. et al. (2005). Mitogenic influence of human R-spondin 1 on the intestinal epithelium. *Science* **309**, 1256–1259. doi:10.1126/science.1112521
- Kim, K.-A., Zhao, J., Andarmani, S., Kakitani, M., Oshima, T., Binnerts, M. E., Abo, A., Tomizuka, K. and Funk, W. D. (2006). R-Spondin proteins: a novel link to beta-catenin activation. *Cell Cycle* **5**, 23–26. doi:10.4161/cc.5.1.2305
- Kimelman, D. and Kirschner, M. (1987). Synergistic induction of mesoderm by FGF and TGF- β and the identification of an mRNA coding for FGF in the early *Xenopus* embryo. *Cell* **51**, 869–877. doi:10.1016/0092-8674(87)90110-3
- Koo, B.-K., Spit, M., Jordens, I., Low, T. Y., Stange, D. E., van de Wetering, M., van Es, J. H., Mohammed, S., Heck, A. J. R., Maurice, M. M. et al. (2012). Tumour suppressor RNF43 is a stem-cell E3 ligase that induces endocytosis of Wnt receptors. *Nature* **488**, 665–669. doi:10.1038/nature11308
- LaBonne, C., Burke, B. and Whitman, M. (1995). Role of MAP kinase in mesoderm induction and axial patterning during *Xenopus* development. *Development* **121**, 1475–1486. doi:10.1016/0168-9525(96)81381-3
- Lowther, W., Wiley, K., Smith, G. H. and Callahan, R. (2005). A new common integration site, Int7, for the mouse mammary tumor virus in mouse mammary tumors identifies a gene whose product has furin-like and thrombospondin-like sequences. *J. Virol.* **79**, 10093–10096. doi:10.1128/JVI.79.15.10093-10096.2005
- Mohammadi, M., McMahon, G., Sun, L., Tang, C., Hirth, P., Yeh, B. K., Hubbard, S. R. and Schlessinger, J. (1997). Structures of the tyrosine kinase domain of fibroblast growth factor receptor in complex with inhibitors. *Science* **276**, 955–960. doi:10.1126/science.276.5314.955
- Nam, J.-S., Park, E., Turcotte, T. J., Palencia, S., Zhan, X., Lee, J., Yun, K., Funk, W. D. and Yoon, J. K. (2007). Mouse R-spondin2 is required for apical ectodermal ridge maintenance in the hindlimb. *Dev. Biol.* **311**, 124–135. doi:10.1016/j.ydbio.2007.08.023
- Nieuwkoop, P. D. and Faber, J. (1967). *Normal Table of Xenopus laevis* (Daudin). Amsterdam: North Holland.
- Northrop, J. L. and Kimelman, D. (1994). Dorsal-ventral differences in Xcad-3 expression in response to FGF-mediated induction in *Xenopus*. *Dev. Biol.* **161**, 490–503. doi:10.1006/dbio.1994.1047
- Ohkawara, B., Glinka, A. and Niehrs, C. (2011). Rspo3 binds syndecan 4 and induces Wnt/PCP signaling via clathrin-mediated endocytosis to promote morphogenesis. *Dev. Cell* **20**, 303–314. doi:10.1016/j.devcel.2011.01.006
- Ornitz, D. M. and Itoh, N. (2015). The Fibroblast Growth Factor signaling pathway. *Wiley Interdiscip. Rev. Dev. Biol.* **4**, 215–266. doi:10.1002/wdev.176
- Patel, A. L. and Shvartsman, S. Y. (2018). Outstanding questions in developmental ERK signaling. *Development* **145**, dev143818. doi:10.1242/dev.143818
- Peng, H. B. (1991). *Xenopus laevis*: practical uses in cell and molecular biology. Solutions and protocols. *Methods Cell Biol.* **36**, 657–662. doi:10.1016/S0091-679X(08)60301-5
- Rapraeger, A. C., Krufka, A. and Olwin, B. B. (1991). Requirement of heparan sulfate for bFGF-mediated fibroblast growth and myoblast differentiation. *Science* **252**, 1705–1708. doi:10.1126/science.1646484
- Raslan, A. A. and Yoon, J. K. (2019). R-spondins: multi-mode WNT signaling regulators in adult stem cells. *Int. J. Biochem. Cell Biol.* **106**, 26–34. doi:10.1016/j.biocel.2018.11.005
- Sato, T., Vries, R. G., Snippert, H. J., van de Wetering, M., Barker, N., Stange, D. E., van Es, J. H., Abo, A., Kujala, P., Peters, P. J. et al. (2009). Single Lgr5 stem cells build crypt-villus structures in vitro without a mesenchymal niche. *Nature* **459**, 262–265. doi:10.1038/nature07935
- Seshagiri, S., Stawiski, E. W., Durinck, S., Modrusan, Z., Storm, E. E., Conboy, C. B., Chaudhuri, S., Guan, Y., Janakiraman, V., Jaiswal, B. S. et al. (2012). Recurrent R-spondin fusions in colon cancer. *Nature* **488**, 660–664. doi:10.1038/nature11282
- Slack, J. M. W., Darlington, B. G., Heath, J. K. and Godsave, S. F. (1987). Mesoderm induction in early *Xenopus* embryos by heparin-binding growth factors. *Nature* **326**, 197–200. doi:10.1038/326197a0
- Smith, J. C., Price, B. M. J., Green, J. B. A., Weigel, D. and Herrmann, B. G. (1991). Expression of a *Xenopus* homolog of Brachyury (T) is an immediate-early response to mesoderm induction. *Cell* **67**, 79–87. doi:10.1016/0092-8674(91)90573-H
- Taniguchi, K., Ayada, T., Ichiyama, K., Kohno, R.-I., Yonemitsu, Y., Minami, Y., Kikuchi, A., Maehara, Y. and Yoshimura, A. (2007). Sprouty2 and Sprouty4 are essential for embryonic morphogenesis and regulation of FGF signaling. *Biochem. Biophys. Res. Commun.* **352**, 896–902. doi:10.1016/j.bbrc.2006.11.107
- Tatsumi, Y., Takeda, M., Matsuda, M., Suzuki, T. and Yokoi, H. (2014). TALEN-mediated maturation in zebrafish reveals a role for r-spondin 2 in fin ray and vertebral development. *FEBS Lett.* **588**, 4543–4550. doi:10.1016/j.febslet.2014.10.015
- Theodorou, V., Kimm, M. A., Boer, M., Wessels, L., Theelen, W., Jonkers, J. and Hilken, J. (2007). MMTV insertional mutagenesis identifies genes, gene families and pathways involved in mammary cancer. *Nat. Genet.* **39**, 759–769. doi:10.1038/ng2034
- Turner, N. and Grose, R. (2010). Fibroblast growth factor signalling: from development to cancer. *Nat. Rev. Cancer* **10**, 116–129. doi:10.1038/nrc2780
- Umbhauer, M., Marshall, C. J., Mason, C. S., Old, R. W. and Smith, J. C. (1995). Mesoderm induction in *Xenopus* caused by activation of MAP kinase. *Nature* **376**, 58–62. doi:10.1038/376058a0
- Wittler, L., Shin, E.-H., Grote, P., Kispert, A., Beckers, A., Gossler, A., Werber, M. and Herrmann, B. G. (2007). Expression of Msn1 in the presomitic mesoderm is controlled by synergism of WNT signalling and Tbx6. *EMBO Rep.* **8**, 784–789. doi:10.1038/sj.embor.7401030
- Yamada, W., Nagao, K., Horikoshi, K., Fujikura, A., Ikeda, E., Inagaki, Y., Kakitani, M., Tomizuka, K., Miyazaki, H., Suda, T. et al. (2009). Craniofacial malformation in R-spondin2 knockout mice. *Biochem. Biophys. Res. Commun.* **381**, 453–458. doi:10.1016/j.bbrc.2009.02.066
- Yayon, A., Klagsbrun, M., Esko, J. D., Leder, P. and Ornitz, D. M. (1991). Cell surface, heparin-like molecules are required for binding of basic fibroblast growth factor to its high affinity receptor. *Cell* **64**, 841–848. doi:10.1016/0092-8674(91)90512-W
- Zhang, M., Zhang, P., Liu, Y., Lv, L., Zhang, X., Liu, H. and Zhou, Y. (2017). RSPO3-LGR4 regulates osteogenic differentiation of human adipose-derived stem cells via ERK/FGF signalling. *Sci. Rep.* **7**, 42841. doi:10.1038/srep42841

Supplementary Material

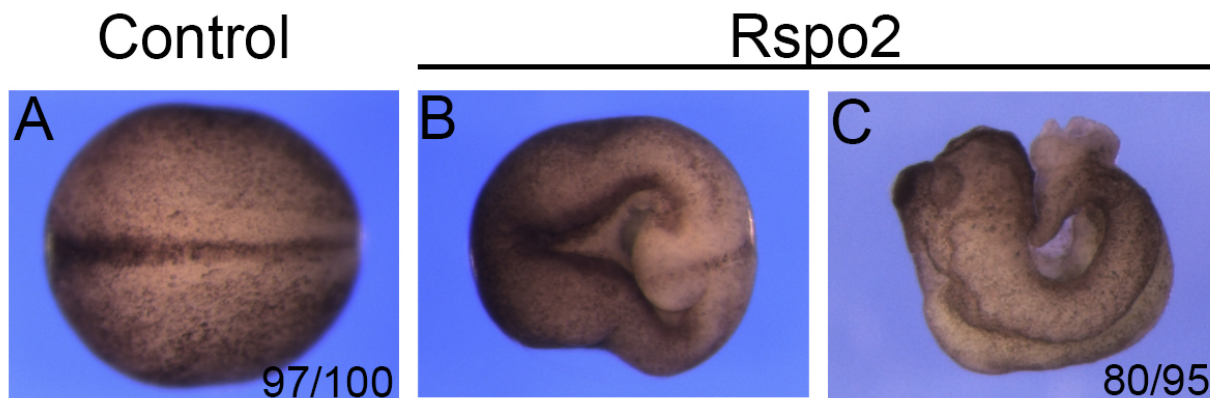


Fig. S1. Phenotypes of embryos injected with Rspo2 RNA.

Four-cell stage embryos were injected into two dorsal blastomeres with Rspo2 RNA (0.5 ng) and allowed to develop until neurula (A, B) or tailbud (C) stages. (A) Uninjected control embryo, stage 19. (B-C) Rspo2-expressing embryos. Open blastopore and posterior defects are apparent. Representative embryos are shown, with more than 20 embryos per group from five separate experiments. The number of embryos displaying the phenotype and the total number of embryos are indicated.

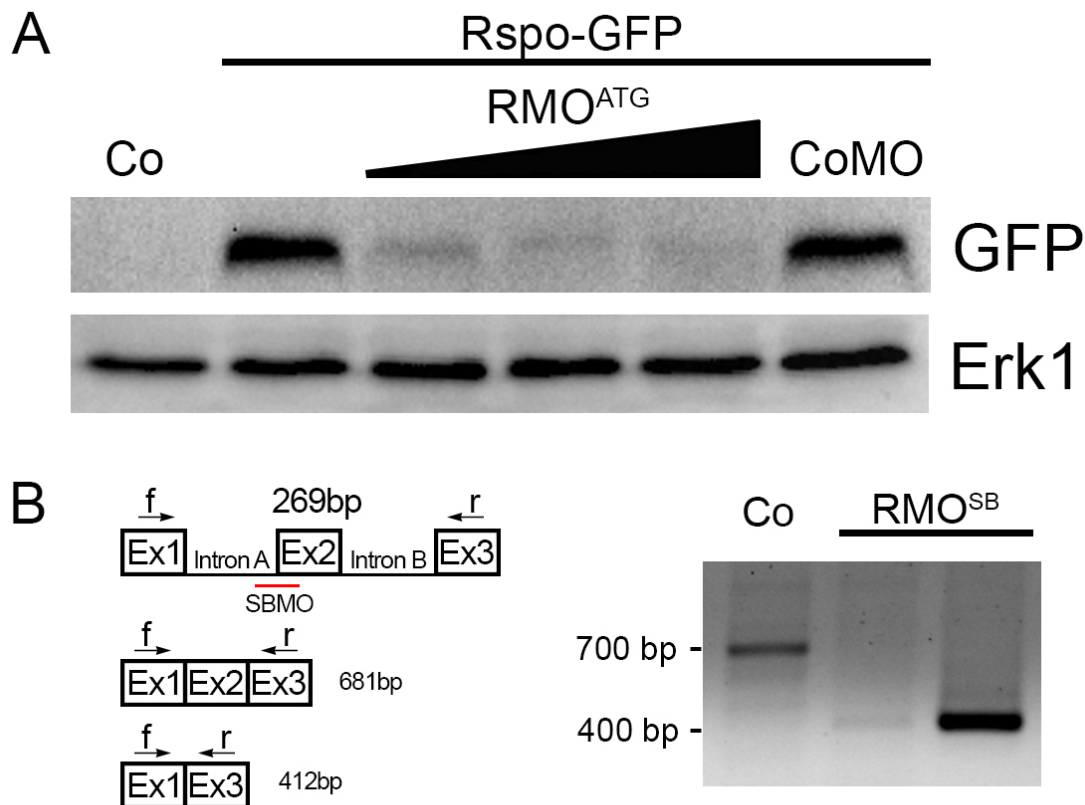


Fig. S2. Validation of Rspo2 knockdown *in vivo*. A, Embryos were injected with Rspo2-GFP RNA (500 pg) alone or coinjected with increasing amounts of RspoMO^{ATG} (10, 20, and 30 ng). Lysates were prepared from injected embryos at stage 11 for immunoblotting with anti-GFP antibody. CoMO (control MO). Co, control uninjected embryo. Erk1 is a control for loading. B, Schematic of RT-PCR to detect changes in Rspo2 RNA splicing. The PCR fragment of 681 bp corresponds to three exons expected in a control embryo. The 412 bp DNA fragment is expected for Rspo2.L RNA with un-spliced exon 2. RT-PCR was carried out with RNA prepared from stage 11 embryos previously injected with RspoMO^{SB} (20 ng). PCR fragments corresponding to a control embryo (Co) and two different embryos injected with RspoMO^{SB} are shown.

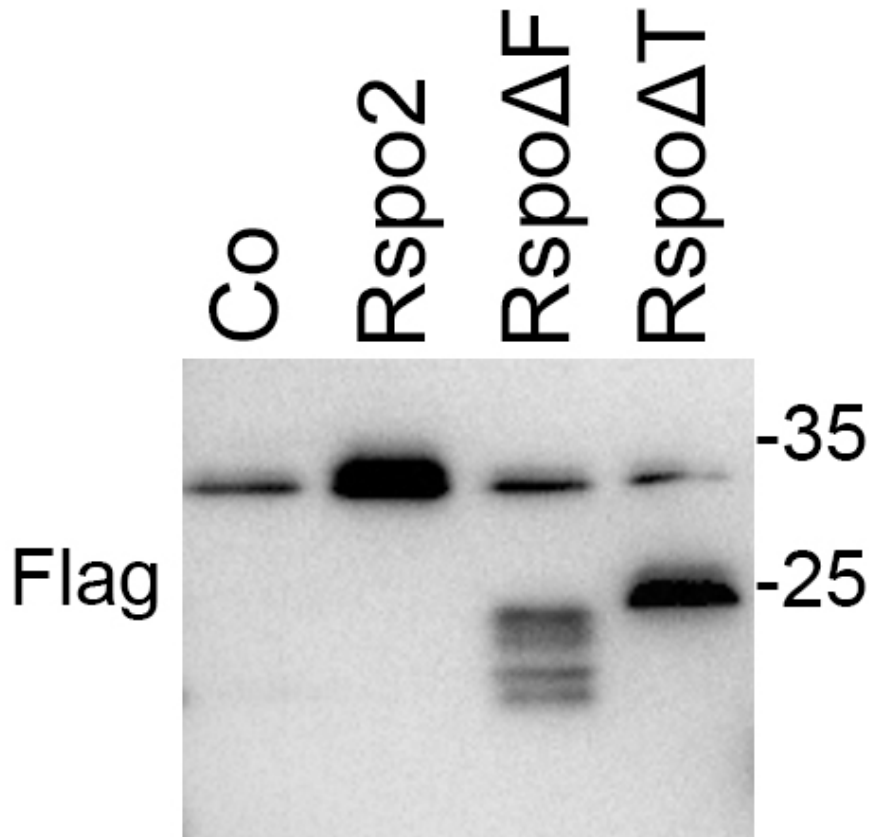


Fig. S3. Expression levels of Rspo2 constructs. RNAs encoding different Flag-tagged Rspo2 constructs (see Fig. 3A) were injected into four cell embryos, ectoderm explants were isolated at midblastula stages and cultured until stage 11 for immunoblotting with anti-Flag antibody.

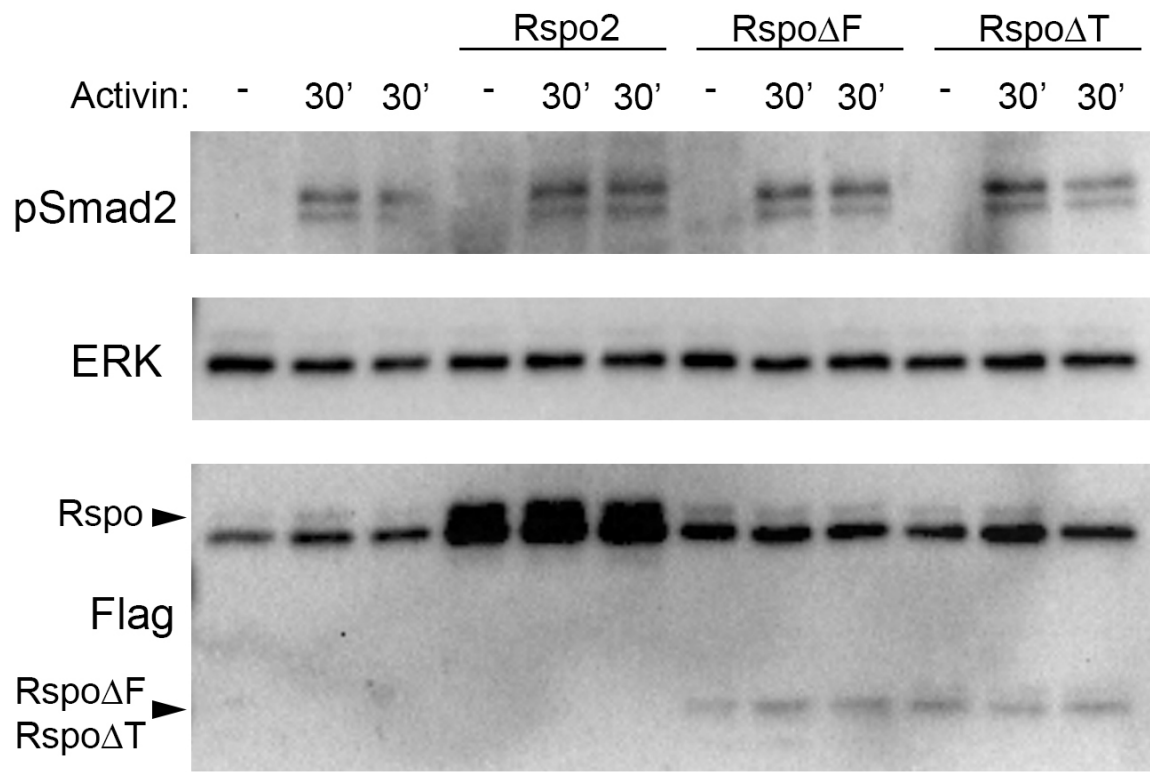


Fig. S4. Lack of Rspo2 effects on Activin/Nodal signaling. RNAs encoding different Flag-tagged Rspo2 constructs were injected into four cell embryos, ectoderm explants were isolated at midblastula stages and stimulated with 0.5 ng/ml of Activin A for 30'. Cell lysates were separated by PAGE and immunoblotted with anti-phospho-Smad2 and anti-Flag antibody.

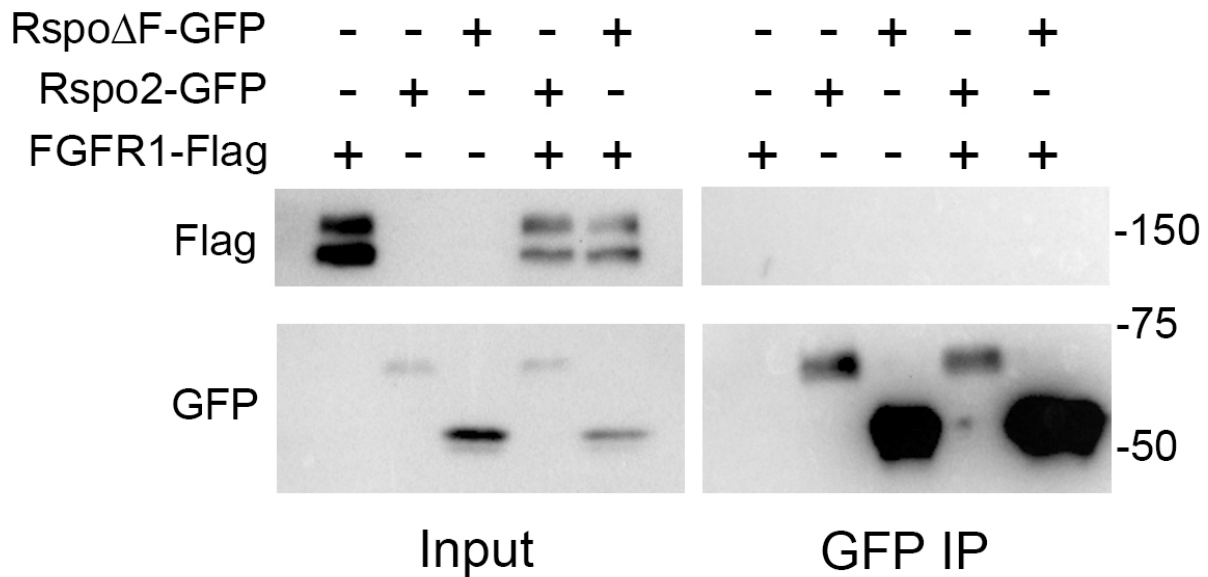


Fig. S5. Lack of Rspo2 association with FGFR1. RNAs encoding different GFP-tagged Rspo2 constructs and/or FGFR1-Flag were injected into four-cell embryos, ectoderm explants were isolated at midblastula stages and cultured until stage 12 for immunoprecipitation (IP) with GFP. FGFR1 is not pulled down with Rspo2-GFP or RspoΔF-GFP.

Table S1.

Primers for cloning Rspo2 cDNA

F: 5'- AGCGAATTCATGCAGTTTCAACTCTTTTC – 3'

R: 5'-TCAGGATCCAGTTGGCTGGACCGGTCTGTAG – 3'

Primers for Rspo2 cDNA mutagenesis

Rspo Δ F:

5'- AGACGGAGCAAGAGAGCCAGATCTCCATTGGATGACACCATG-3'

Rspo Δ T:

5'-TGC GTGGATGGCTGTGAAGCTAGCGGAGGAACAAGAACCACA-3'

Primers for RT-qPCR

<i>cdx4.L:</i>	Forward: 5'-TGATTTATCACCTAACCAG-3'
	Reverse: 5'-GTCCCAGATGGATGAGGAGA-3'
<i>eef1a1.S:</i>	Forward: 5'-ACCCTCCTCTTGGTCGTTTT-3'
	Reverse: 5'-TTTGGTTTTTCGCTGCTTTCT-3'
<i>tbxt.S:</i>	Forward: 5'-TCACTAGCCATTCATTCCCT-3'
	Reverse: 5'-GACTATCGATTCCCTCATCC -3'
<i>msgn1.L</i>	Forward: 5'-GTATCCAACACTTTGCCATG-3'
	Reverse: 5'-AGCACTGGAGAAGGTTTGTG-3'